CrossMark

ORIGINAL PAPER

Ability of Two Dam Fine-Grained Sediments to be Used in Cement Industry as Raw Material for Clinker Production and as Pozzolanic Additional Constituent of Portland-Composite Cement

Antoine Faure[1,2] · Agnès Smith[2] · Coryse Coudray[1] · Baptiste Anger[1] ·
Horacio Colina[3] · Isabelle Moulin[4] · François Thery[1]

Abstract   Fine-grained sediment deposition is a phenomenon that occurs at different extents in all the reservoirs. This particle accumulation has to be properly managed, in accordance with the operational needs and the environment. As an extracted and on-land managed sediment has to be considered as a waste material according to both European and French regulations, sustainable reuse options need to be investigated. One of them could be a beneficial reuse as a raw material in cement industry either as partial substitution in Portland clinker raw mix or as a supplementary cementitious material (SCM) after thermal treatment in order to activate its possible pozzolanic activity. Two dredged materials, labelled SEP and STA, both from French hydroelectric reservoirs, are characterized on physical, chemical and mineralogical aspects. SEP is used as raw material partial replacement for clinker synthesis and the other one is calcined in the range 550–1000 °C aiming to obtain a pozzolanic reactive material that could be used as supplementary cementitious material in blended Portland cement. After thermal treatments, the products are characterized and compared to ordinary Portland cement (OPC) and to pozzolanic active materials (fly ash from pulverized-coal power plant). Results showed that each sediment is suitable for the only tested reuse option. For the clinker prepared with SEP sediment, the morphology and the mineralogical composition correspond to those of a typical Portland clinker. Concerning calcined STA pozzolanic activity, the optimum thermal treatment was found to be 900 °C using the chemical Frattini test. Similar compressive strength results were obtained with calcined STA and silico-aluminous fly ash.
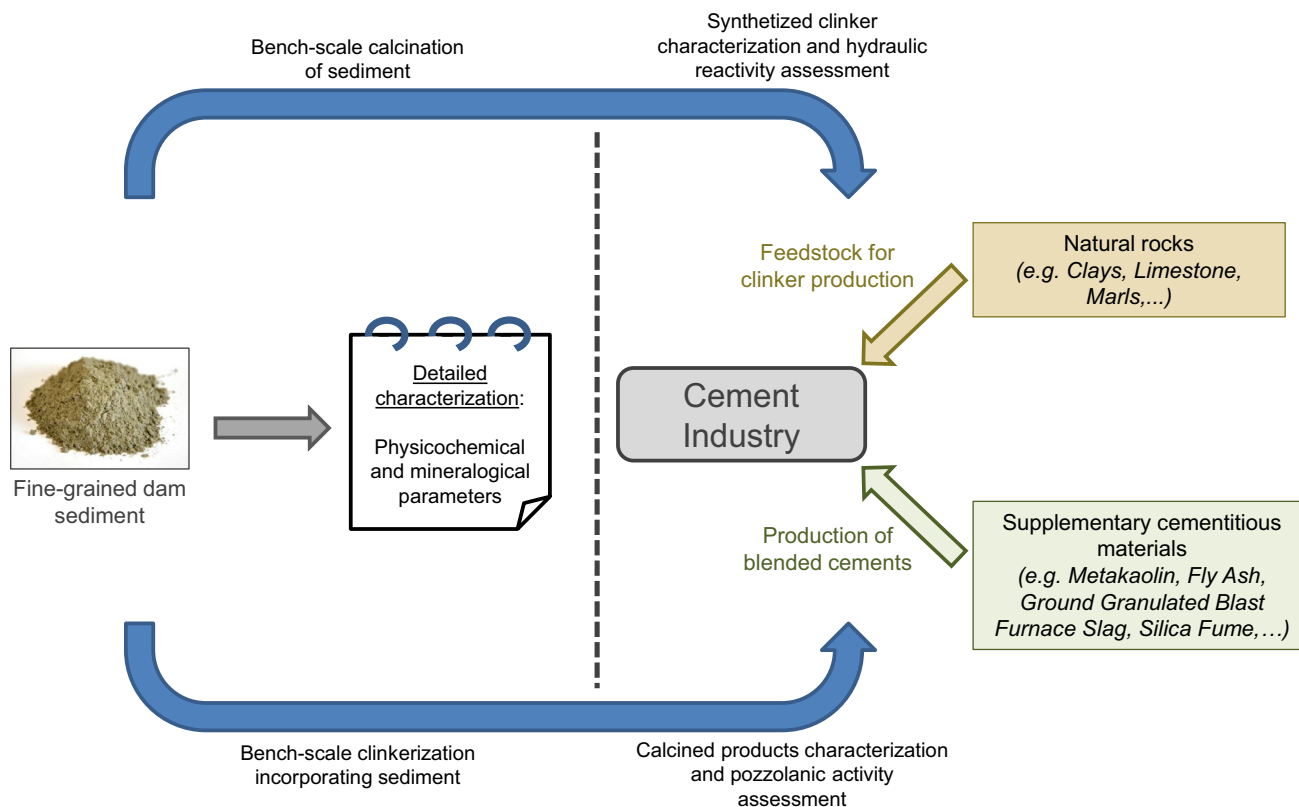
✉ Antoine Faure
  antoine.faure@etu.unilim.fr

[1] EDF R&D, Eco-efficiency and Industrial Process Department, Les Renardières, 77818 Moret-sur-Loing, France

[2] Univ. Limoges, CNRS, ENSCI, SPCTS, UMR 7315, 87000 Limoges, France

[3] ATILH, 92974 Paris-La-Défense, France

[4] LERM, 13631 Arles, France

Graphical Abstract

Introduction

Water reservoirs are built and used for various purposes such as power source, irrigation and drinking water storage. Whatever their use, they are subject to sedimentation phenomena. Accumulation of particles leads to a reduction of the dam capacity and may cause perturbations for hydroelectric dam operators. Sediment yield is spatially and temporally variable [1]. Several factors affect spatial and temporal variations such as geological, topographical and hydro-meteorological features as well as human interventions [2]. Temporal variations are both annual and interannual [3]. Two size fractions can be distinguished in accordance with Wentworth scale as defined by Udden in 1914 [4] and Wentworth in 1922 [5]: (i) coarser particles which are gravels (>2 mm) and sands (between 63 μm and 2 mm) and (ii) the fine-grained materials which are silts (4 μm to 63 μm) and clays (<4 μm) that can remain in suspension even when flow velocity is reduced. Thus, sedimentation phenomena of the finer fractions mainly occur close to the dam structure where the reservoir usually is deeper [6].

In compliance with current environmental legislations concerning water and aquatic environments, an ecological continuum has to be maintained along watercourses [7]. Sufficient sediment transport is part of this continuum. Dam operators are responsible for guaranteeing the sediment transfer downstream [8]. Thus, in conformity with these rules, the major part of the managed dam sediment is transferred from one side of the dam to the other by different means, such as "pumping-dilution" technique.

Nonetheless, due to environmental or technical reasons, hydroelectric dam operators might have to deal with on-land management of sediments. According to European and French regulations, sedimentary material extracted from a watercourse (e.g. in a reservoir) has to be considered as waste [9]. This status has an impact on management solutions: a waste producer should preferentially choose recycling and valorization options instead of landfill option. Different beneficial reuse options can be considered for fine-grained dredged material as summarized by Anger [10]. One of them is a beneficial reuse as a raw material in the cement industry. Due to the important raw material tonnage required in cement plants, this reuse option was chosen for investigation.

Two different binders will be considered: hydraulic and pozzolanic binders. Both of them are finely divided materials. For instance, considering typical Portland cements,

between 7 and 9% of particles are finer than 2 μm and less than 4% are above 90 μm. Thus, around 90% of particles are in the 2–90 μm range [11].

Hydraulic binders, can set and harden when mixed with water. Strength and stability are maintained even under water. Pozzolanic compounds, are able to set and harden if they are mixed with calcium hydroxide in presence of water [12].

In both cases, literature shows that alternative resources, often waste, can be used in a circular economy approach. Using waste material in Portland cement clinker production is a relevant eco-friendly solution: it limits the mineral extraction in quarries and, at the same time, it limits landfilled waste [13]. Blending Portland cement with an alternative pozzolanic material has an additional advantage which is a limitation of carbon dioxide emissions by ton of manufactured cement. Using life-cycle analysis, the CO_2 emission reduction using blended cement was found to be around 22% compared to Ordinary Portland Cement [14] since less clinker is required in the formulation.

In clinker manufacture, it was demonstrated that numerous waste materials could be used as a partial replacement in clinker raw meal. We could mention wastes from building demolition activities [15, 16], the steel and metalworking industry [17, 18], paper industry [19], rock quarrying activity [20], recycled glass [21] and waste generated by communities (sanitation—water treatment [22, 23], and municipal waste management [24, 25]).

Looking for innovative supplementary cementitious materials, it was shown in literature that various waste materials exhibit pozzolanic activities and therefore could be used in blended cements: waste from the ceramic industry (fired clay roof tiles [26] and sanitary ware waste [27]), waste from the paper industry [28, 29], ashes obtained from the calcination of agricultural residues (e.g. sugar cane bagasse [30], rice husk [31, 32], barley husk [32]), thermally activated waste from rock extraction activity [33] or bottom ashes coming from municipal solid waste incineration [34].

Focusing on sediment reuse in the cement industry, some authors have already considered recycling dredged material in Portland cement raw meal or as a pozzolanic addition.

On the Portland clinker aspect, Valenti et al. [35] experimented a total substitution of the argillaceous material by sediments coming from two Italian reservoirs. The initial binary raw meal contained 73.3% limestone and 26.7% clay by mass. The study was mainly focused on the ease of the chemical reactions between the lime obtained after limestone decarbonation and the silica, alumina and iron oxide mainly provided by the fine-grained dam sediment or by the quarried argillaceous rock for the control sample. The oxide combination level assessment was performed using the Burnability Index (BI) value. BI is calculated by Valenti et al. four free lime measurements on clinker after different sintering temperatures in the 1350–1500 °C range. Equation 1 is used.

$$BI = 3.73 \times \frac{(Y + Z + 2T + 3W)}{\sqrt[4]{Y - W}} \tag{1}$$

where Y; Z; T and W correspond to the free lime content at 1350, 1400, 1450 and 1500 °C, respectively.

It was shown by Valenti et al. that BI values were within the 11.29–50.87 range, which is lower than 60 as recommended. Thus, burn abilities of the clinkers prepared with sediment were considered as acceptable, even if they were slightly more difficult to sinter than a traditional meal.

Dalton et al. [36] synthetized clinkers substituting industrially quarried rocks with sediments from US marine harbors both at the lab scale and at the industrial pilot scale using a cement plant rotary kiln. In the industrial pilot, 6.5% by mass of raw sediment were incorporated into the mixture. They produced Portland cement that complied with ASTM C150 requirements [37], even if mechanical strengths were slightly lower than the Portland cement control samples. This observation was mainly attributed by the authors to the lower alite-to-belite ratio of the clinker that incorporate alternative raw materials. Authors pointed out the required rapid cooling in order to maintain a satisfying alite-to-belite ratio even at laboratory scale. Aouad et al. [38] incorporated 39% of siliceous sediment extracted from a French canal. Anhydrous clinker phases synthetized at laboratory scale, particularly calcium silicates, were found to be more reactive than calcium silicates of a commercial OPC (CEM I 52.5). It was shown by isothermal calorimetry that hydration reactions of the alternative cement were faster. These results were well correlated to mechanical strengths tests: at 28 days, strengths developed by the Portland cement prepared with dredged material was higher than the commercial CEM I 52.5.

On the pozzolanic activity aspect, four main references can be identified in literature. Semcha in 2006 [39] calcined fine-grained sediments from the Algerian reservoir of Fergoug at 750 °C. A transformation of the kaolinite—the main clay mineral of the deposit—to metakaolinite was expected. This amorphous phase is assumed to react with calcium hydroxide. Semcha showed that it is possible to substitute 30% of CEM I Portland cement by calcined sludge without any loss in unconfined compression strength. Later, Dang et al. [40] fired estuarine fine-grained sediment at 650 and 850 °C. It was demonstrated that a thermal treatment at 650 °C gives the best results for mechanical compression tests. Even if mechanical performances are lower than those of the control CEM I, blended cements containing up to 33% could integrate the 42.5 MPa

strength class. Furthermore, Rabehi et al. [41] showed that the use as a supplementary cementitious material of fine-grained sediment from an Algerian dam and calcined at 750 °C modifies the microstructure of the cement pastes and mortars. As the mortars are less porous and denser, they were less sensitive to chloride ion penetration and to sulfatic acid attack than the mortars containing only Ordinary Portland Cement (OPC). The chosen replacement level was 10%. Finally, Snellings et al. [42] showed that flash-calcined sediment extracted from Antwerp port are pozzolanically active. Three calcination temperatures were tested between 820 and 905 °C. Pozzolanic reaction is known to be exothermic. Therefore, released heat by mixes containing $Ca(OH)_2$, Supplementary Cementitious Materials (SCM) and water is followed during 5 days. Results are interpreted saying that the higher the released heat, the more reactive the supplementary cementitious material is. No significant variability is observed according to the calcination temperature. All the calcined sediments are found to be more reactive than comparative fly ash and inert powdered quartz but less pozzolanic than metakaolin using this calorimetry test.

Case studies from literature with partial replacements of cement industry raw materials by fine-grained sediment showed satisfying results. However, a few number of studies concern reservoir fine-grained sediment. Moreover, due to the variability in mineral and chemical composition, each waste has to be carefully characterized before identifying their substitution potential.

The first aim of this manuscript is to present a characterization of two fine-grained sediments named SEP and STA sampled by EDF Group in hydroelectric reservoirs, located in the French Alps area and in Brittany region, respectively.

Two reuse options are then considered: on one hand using the sediment as partial replacement in raw material mixture for clinker manufacture and, on the other hand, using it as Supplementary Cementitious Materials. After the characterizations of each dredged material that are developed below, it appeared that the first one had chemical characteristics more promising for the clinker raw mix reuse option while STA seemed more suitable for calcination and reuse as SCM.

Then, SEP sediment is tested as an alternative to clay rock in an industrial clinker raw meal. Clinker characteristics are analyzed and compared to those of an OPC. Concerning the reuse of calcined STA as SCM, the optimal thermal treatment is not known in advance. 10 different calcination temperatures are tested in the 550–1000 °C range. For each temperature, the calcination product is characterized and pozzolanic activity is assessed.

Both these approaches are relevant in waste management by limiting disposal. This paper investigates the technical and scientific feasibilities with bench scale experiments.

Sediment Samples

Materials and Methods

Both the studied sediments named SEP and STA – were sampled by EDF Group in hydroelectric reservoirs, located in the French Alps area and in the Brittany region, respectively. STA was sampled using a Van Veen grab sampler whereas SEP sampling was performed during a low reservoir level period with a mechanical shovel. SEP was tested as partial replacement of clinker raw material while STA was investigated as a supplementary cementitious material after thermal treatment.

For clinker beneficial reuse, raw materials coming from cement plant quarries were used: two types of limestone and one clay rock in order to meet the specifications of the industrial meal formulation.

Prior to characterizations, the raw materials underwent a preliminary treatment. They were dried at 40 °C to get a constant mass. Due to the relatively high clay minerals content, this drying step led to the formation of tight clusters that had to be crushed to obtain the actual particles. The evolution of the material state during the pre-treatment step is presented in Fig. 1, with STA.

Raw sediments that underwent drying and crushing operations will be named "pre-treated sediments" in the following sections.

Physical Characterization

Particle size distributions (PSD) were analysed by laser diffractometry using a Malvern Instruments Mastersizer 2000 apparatus after a liquid and ultrasonic dispersion.

Specific surface areas (SSA), according to Brunauer–Emmett–Teller (BET) theory [43], were measured with a Micromeritics Tristar II device. Outgassing operations lasted 17 h at a temperature of 120 °C. N_2 was used as adsorbate.

Blaine fineness was assessed by air permeability technique [44] according to EN NF 196-6 standard [45]. It consists in measuring the time needed to transfer a known air volume through a compact of cement. This duration is related to the resistance of the cement to air flow [46], in relation with the specific surface area of particles and their fineness.

Finally, densities are obtained by the helium pycnometry technique with a Micromeritics Accupyc 1330 device.

Chemical Characterization

Chemical compositions of sediments were obtained by ICP-AES technique after an alkali-fusion digestion. Measures were made on a Varian apparatus.

Fig. 1 Sediment state evolution during the pre-treatment step

Mineralogical Characterization

Crystalline phases contained in sediment samples were analyzed by X-Ray Diffraction, on a Bruker D8 ADVANCE device mounted on a Bragg–Brentano geometry, equipped with a Cu anticathode ($\lambda = 1.5406$ Å) and operating at 40 kV and 40 mA. Angles between 5° and 70° 2θ were analyzed with a step of 0.02° 2θ. After the acquisition, XRD patterns were processed using the Bruker DIFFRAC^{plus} EVA software allowing the identification of crystalline phases (PDF-4 + 2015 database from the International Center for Diffraction Data). Phase quantification was performed using the Bruker TOPAS software. Pre-treated sediments and calcined STA amorphous contents were estimated using the internal standard technique with zinc oxide as internal standard. The known internal standard mass allows the calculation of the amorphous content with Eq. 2 [47].

$$X_a = \frac{100}{(100 - X_s)} \cdot \left(1 - \frac{X_s}{X_{s,c}}\right) \tag{2}$$

where X_a is the calculated amorphous weight fraction, X_s is the known weight fraction of internal standard added to the analyzed powder (10 wt% in the study) and $X_{s,c}$ is the estimated weight fraction of internal standard by Rietveld refinement.

Additionally, carbonate and organic matter contents were assessed according to NF P94-048 standard (Bernard calcimeter technique) [48] and NF EN 12880 loss on ignition method [49], respectively.

Thermal Analysis

Thermal behaviours of dredged materials were analysed by simultaneous thermogravimetry and differential thermal analysis (TGA-DTA) on a Setaram Setsys 16/18 TG-DTA device. Thermal cycles were similar for both the sediments: a heating ramp of 5 °C/min until 1000 °C followed by a cooling ramp of 10 °C/min.

Scanning Electron Miscoscopy

Powder mounts of both SEP and STA were observed by Scanning Electrode Microscopy (SEM) using a field-emission environmental FEI Quanta 450 apparatus.

Sediment Characteristics and Discussion

Physical properties are presented in Table 1 along with carbonate and organic matter measurement results. PSD curves are given in Fig. 2.

The physical parameters are variable between pre-treated SEP and STA. The BET specific surface area of SEP is relatively low compared to STA. It suggests that particles of SEP have a low surface roughness. It could be directly related to the mineral composition. The high SEP carbonate content (calcite and dolomite) presented

Table 1 Properties of the studied pre-treated sediments

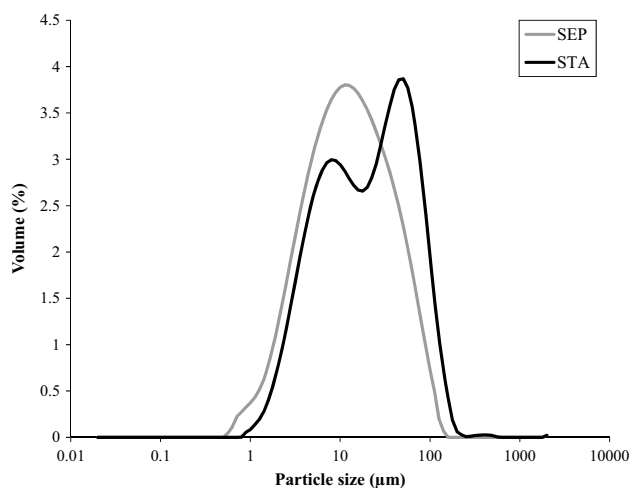| Property	SEP	STA
Density (g/m^3)	2.79	2.51
BET SSA (m^2/g)	5.17	8.92
Blaine fineness (cm²/g)	7547	7611
d$_{10}$ (µm)	3.0	4.1
d$_{50}$ (µm)	12.9	21.7
d$_{90}$ (µm)	53.8	81.8
Carbonate content (wt%)	30.1	4.4
OM content (wt%)	1.0	8.4

Fig. 2 Particle size distributions of pre-treated SEP and STA sediments

in Table 1 tends to diminish the global BET SSA of the material. Contrary to BET technique, Blaine SSA are similar for pre-treated STA and SEP. Thus, BET and Blaine techniques do not give similar information. As shown by Michel and Courard on limestone fillers, BET and Blaine methods should be seen as two complementary techniques [50]. BET is known to be more influenced than the air-permeability methodology by surface roughness, open

porosity and micro-cracks [11, 51]. Considering helium pycnometry density value, it can be observed that SEP is denser than STA. This parameter could be related to the organic matter (OM) content. Indeed, a density of 2.51 is lower than the individual densities of the minerals composing the sediment. Thus, an explanation of this global low density would be the OM weight fraction.

Finally, Fig. 2 shows that the SEP sediment has a Gaussian distribution centered at 12 μm whereas STA shows a bimodal density curve. The first peak is located at 8 μm and the second one, around 50 μm. These distributions can be completed by the d_{10}, d_{50} and d_{90} values: all of them are higher for STA than for SEP, especially the d_{90} value. The differences observed in particle size distribution suggest that SEP is relatively homogeneous.

XRD patterns of pre-treated SEP and STA sediments are presented in Fig. 3. The main mineral phases are identified and XRD quantifications are given in Table 2. Chemical compositions of both materials are given in Table 3. These compositions are plotted in the silica-alumina-lime ternary phase diagram (Fig. 4), also named Rankin-Wright diagram [52]. According to Aïtcin [53], chemical compositions of several cementitious materials that contain silica, lime and alumina as main oxides are also showed in Fig. 4.

In correlation with the differences observed for mineral compositions, STA and SEP have rather different chemical composition. Although silica is the main oxide
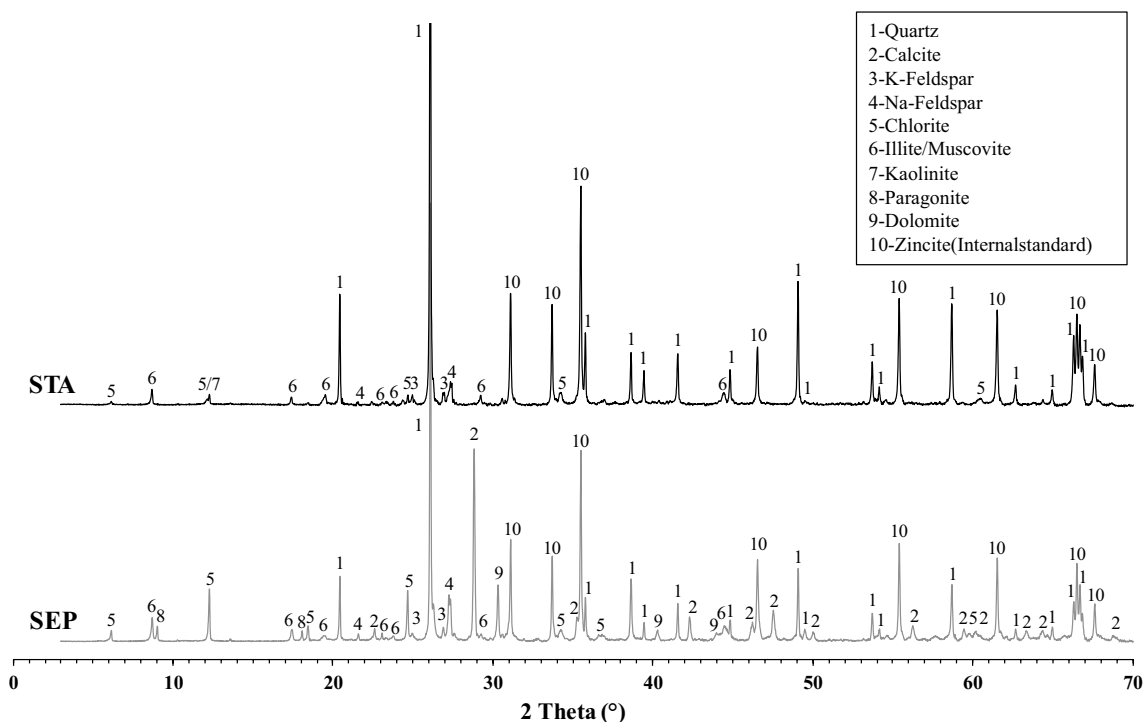

Fig. 3 XRD patterns of pre-treated STA and SEP sediments

Table 2 Pre-treated sediments mineralogical analysis

Mineral	STA (wt%)	SEP (wt%)
Quartz	59.1	22.4
Illite	4.0	9.8
Kaolinite	1.4	–
Chlorite	0.2	0.5
Muscovite	18.7	17.6
Paragonite	–	5.6
K-feldspar	12.9	2.5
Na-feldspar	3.7	11.9
Ca, Mg carbonates	–	29.7

Table 3 Pre-treated sediments chemical analysis

	STA (wt.%)	SEP (wt%)
LOI	10.0	18.6
SiO_2	67.9	44.4
Al_2O_3	11.6	11.3
Fe_2O_3	4.4	4.5
CaO	1.5	15.4
MgO	0.7	3.6
Na_2O	0.5	0.9
K_2O	2.0	2.3
SO_3	0.1	–
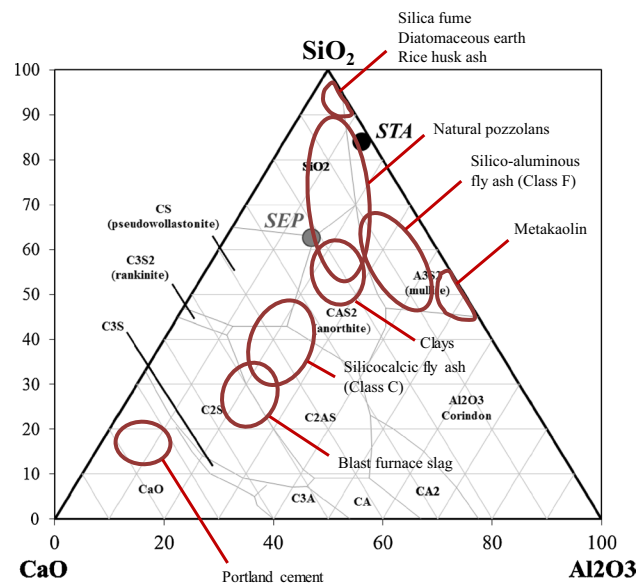
Fig. 4 SEP and STA chemical compositions in Rankin-Wright diagram

for both the dredged material (over 44%), explaining that all of them are located in the upper part of the ternary phase diagram, the ratio CaO/SiO_2 is higher for SEP than for STA. It can be directly associated to the calcium carbonate content that is almost null for STA. The other carbonate contained in SEP, dolomite—$CaMg(CO_3)_2$, is also an explanation to CaO and MgO weight fractions. The very high content in silica for STA, close to 70%, could be related to both the presence of quartz and phyllosilicates.

Comparing in Fig. 4 the positions of the dots representing SEP and STA to the areas defined by [53], it can be shown that STA is very close to the ellipses that correspond to natural pozzolan and silica fumes, an artificial pozzolan resulting from silicon industry [54]. Moreover, the absence of carbonates—that could have detrimental effects on reactivity when CaO and MgO are formed after decarbonation—is an advantage in pozzolanic reactivity development after an optimized thermal treatment. On the other hand, SEP sediment is located close to the "clay" area. Because SiO_2 content is the main oxide, with a non-negligible percentage of Al_2O_3, a partial replacement of quarried clay by SEP in clinker raw mix can be suggested. Furthermore, since the lime content is over 15%, the incorporation of limestone could also be reduced using this fine-grained sediment.

Results of simultaneous TG-DT analyses are shown in Fig. 5 and mass losses in the temperature range 105–1000 °C are detailed in Table 4. In order to avoid the influence of the varying free water content, the total mass loss is calculated using the mass at 105 °C as the zero reference.

As a comment of combined TG/DT analyses, it can be said that the obtained results are consistent with what was previously observed:

- High content of organic matter for STA resulting in a marked exothermic peak around 300 °C due to its oxidation;
- Noticeable endothermic peak for SEP between 750 and 800 °C attributed to loss of CO_2 by carbonates (corresponding to a mass loss over 10%);
- Concerning phyllosilicates, many overlaps exist in the 400–800 °C temperature range.
- Thermal characterizations are in accordance with carbonate and OM assessments with other techniques (Table 1).

SEM observations of pre-treated SEP and STA are presented in Fig. 6.

In both cases, SEM observations demonstrated that particles are usually a mix of several mineral species (phyllosilicates, quartz, feldspars and, for SEP, calcite). Only in STA powder, biogenic particles, mainly diatoms, can often be identified (e.g. bottom-right corner of micrograph).

Fig. 5 Combined TG-DT analyses of pre-treated SEP and STA from room temperature to 1000 °C *Continuous lines:* DTG, *Dotted lines*: TGA
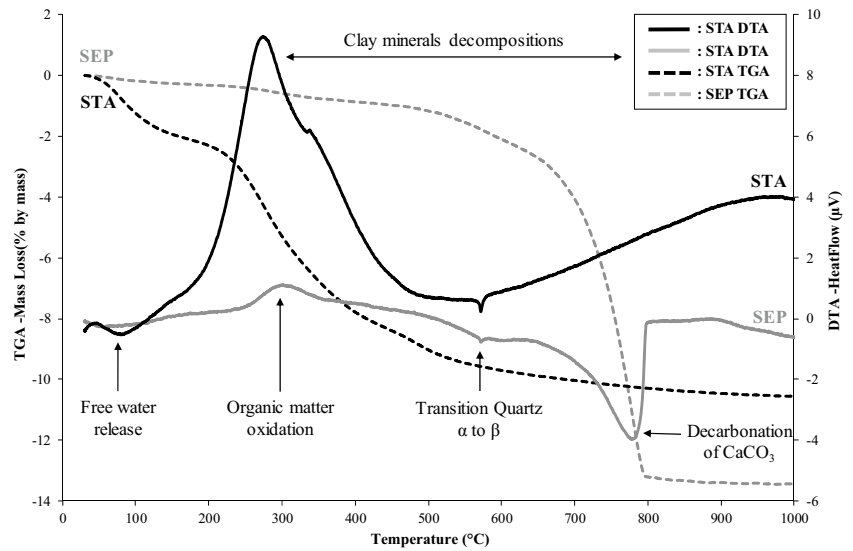

Table 4 Summary of mass losses in thermogravimetry in the temperature range 105–1000 °C

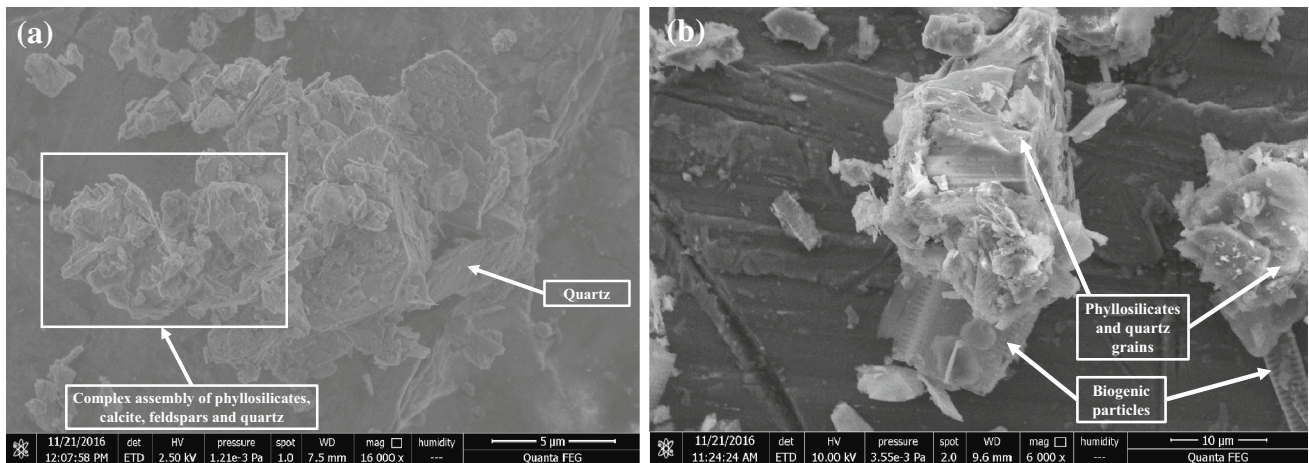| Temperature range (°C)	Mass loss SEP (%)	Mass loss STA (%)	Fact and observations
105–450	0.79	7.05	Remaining adsorbed water and organic matter oxidation
450–650	1.73	1.48	Kaolinite and chlorite dehydroxylation
650–800	10.48	0.41	Calcite and dolomite decarbonation
800–1000	0.22	0.26	Remaining phyllosilicates dehydroxylation
Total	13.22	9.20	

Fig. 6 SEM observations of pre-treated SEP (**a**) and STA (**b**)

Table 5 Quarried material chemical analysis

	LS1 (wt%)	LS2 (wt%)	Clay (wt%)
LOI	42.63	36.30	18.27
SiO$_2$	1.49	21.15	43.62
Al$_2$O$_3$	0.54	3.62	11.16
Fe$_2$O$_3$	1.07	2.95	4.38
CaO	52.74	42.34	18.68
MgO	0.43	1.18	1.10

Table 6 Main clinker phases chemical formulae according to the cement nomenclature

Phase name	Full chemical expression	Cement nomenclature
Alite	3 CaO.SiO$_2$	C$_3$S
Belite	2 CaO.SiO$_2$	C$_2$S
Celite	3 CaO.Al$_2$O$_3$	C$_3$A
Felite	4 CaO.Al$_2$O$_3$.Fe$_2$O$_3$	C$_4$AF

Note: In hydrated phases, H$_2$O is usually abbreviated H

e.g. C–S–H refers to hydrated calcium silicate

Clinker Reuse Option

Materials and Methods

Raw Meal Design

Chemical composition of the partially substituted quarried rocks are given in Table 5.

Raw meal was designed using two cement manufacturing parameters: Lime Saturation Factor (LSF) and Silica Ratio (SR). These moduli are calculated according to the following (Eqs. 3 , 4):

$$LSF = \frac{\% \, CaO}{2,8 \times \% \, SiO_2 + 1,18 \times \% \, Al_2O_3 + 0,65 \times \% \, Fe_2E_3} \quad (3)$$

$$SR = \frac{\% \, SiO_2}{\% \, Al_2O_3 + \% \, Fe_2O_3} \quad (4)$$

In equations (3) and (4), the mass percentage of each oxide is considered. The targeted values for these cement industry parameters were LSF = 98.5 and SR = 2.4. They were chosen in accordance with industrial requirements for clinker production [55]. The chemical compositions of (i) the quarried natural resources and (ii) the dam sediment

allowed to solve the equations and to determine the weight fraction of traditional and alternative raw materials in the mix.

In the next sections, nomenclature from the cement chemistry is used. Each oxide is abbreviated by one capital letter: C, S, A and F corresponding to CaO, SiO$_2$, Al$_2$O$_3$ and Fe$_2$O$_3$, respectively. Therefore, the clinker phase chemical formulae can be expressed as the sum of component oxides. According to cement nomenclature, the abbreviations for the four main anhydrous clinker phases are given in the following Table 6.

Preparation of the Clinker Meals and Bench-scale Sintering/clinkerization process

Knowing the content of each raw material, powders were weighted, homogenized and granulated. During this granulation step, the dry raw meal is mixed with water on a disc granulator (water-to-solid ratio equal to 0.22). Then, pellets are dried at 105 °C to obtain a constant mass. Pellets are sintered in an elevator furnace using a platinum crucible. The thermal cycle can be divided into 4 steps. Firstly, the mix is heated from room temperature to 1450 °C with a 20 °C/min ramp. This ramp is followed by a dwell period of 45 min at the maximum temperature. After a ramp of 1 min from 1450 °C to 1350 °C, the crucible is quenched to room temperature. This thermal shock operation is assumed to preserve the unstable phases formed during the clinkerization reactions, particularly the tricalcium silicate phase (C$_3$S). It is known that a slow cooling of clinker nodules can lead to the decomposition of C$_3$S into dicalcium silicate (C$_2$S) and lime (CaO). This reverse reaction is known as resorption of alite [11]. Thus, the quenching step at laboratory scale mimics what is observed in a cement plant since clinker nodules are usually quenched using a grate cooler [56]. Clinker pellets thus obtained were stored in dessicator, to avoid unwanted hydration reactions.

Clinker Characterization

Clinker nodules were observed in polished sections (reflected light microscopy). Before the observation, clinker samples were vacuum impregnated by epoxy resin and polished. Afterwards, polished section were etched by NaOH solution followed by an ethanol-HNO$_3$ solution (nital), in order to successively reveal and color the interstitial aluminates and the silicate phases [57].

Crystalline phase quantification was performed using two methods: counting on polished section with optical microscope and the Rietveld refinement method with the Bruker TOPAS Software.

Before carrying out both the following protocols, it was necessary to grind the clinker nodules. This operation was

Table 7 Raw meal composition with reference and SEP mixtures

Raw material	LS1	LS2	Clay	SEP
Reference mix (wt %)	68.7	3.5	27.8	0.0
Mix with SEP (wt %)	70.4	2.5	0.0	27.1

Note: *LS1* limestone 1, *LS2* limestone 2

Table 8 Mineralogical composition of the clinker prepared with SEP sediment by optical microscopy counting

Clinker phase	C_3S	C_2S	C_3A	C_4AF
Percentage by volume	70.2	10.9	12.2	6.0
Density (g/cm³)	3.15	3.28	3.03	3.80
Percentage by mass	69.2	11.5	11.0	8.3
Usual wt% according to Pliskin [60]	[40; 70]	[0; 30]	[2; 15]	[0; 15]

done using a planetary ball mill. The PSD was controlled: $d_{10} = 0.9$ μm, $d_{50} = 6.7$ μm and $d_{90} = 23.7$ μm. PSD after grinding corresponded to a typical particle distribution in industrial Portland clinker. According to Neville [58], a clinker shows desired early strength if at least 50% of the particles are in the 3–30 μm range. A higher percentage is even better, both for the early strength development and the final strength of the concrete formulated with this cement.

In order to assess the quality of a Portland clinker, an interesting parameter is the free lime content. According to Javellana and Jawed [59], it gives information on the completeness of the clinkering reaction. Lime is extracted from clinker powder by hot ethylene glycol, according to the technique developed by Schläpfer and Bukowski [60]. The suspensions were stirred for 30 min at 70 °C. After vacuum filtration, a colorimetric acid-base titration is performed on two replicates using HCl as titrating solution and bromocresol green as indicator for free lime evaluation.

Results and Discussion

Composition of the Raw Meal

The targeted clinker ratios—LSF = 98.5 and SR = 2.4—give the composition of the meal presented in Table 7. It corresponds to the maximum possible incorporation rate.

It can be seen that, thanks to close chemical compositions between the industrial argillaceous matter and SEP sediment, 100% of the quarried clay rock was substituted by the incorporation of alternative dredged raw material. Of course, lower amounts of sediment could have been incorporated into the clinker raw mix. However, in order to demonstrate how interesting the use of dredged
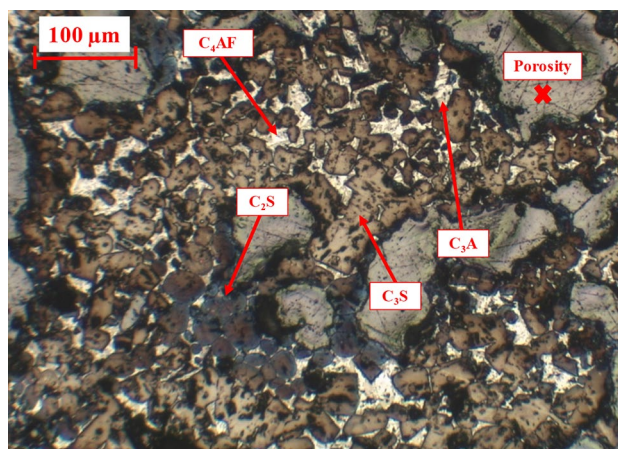
Fig. 7 Polished surface of clinker prepared with SEP sediment (NaOH-ethanol and nital etch)
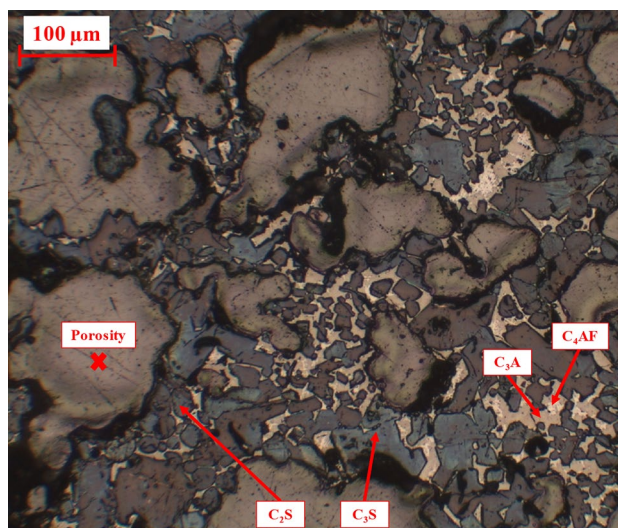
Fig. 8 Polished surface of clinker prepared without SEP sediment (NaOH-ethanol and nital etch)

material for the production of Portland cement is, it is relevant to work on the maximum percentage of sediment that can be integrated into the mix. Then, the next question is: "Do we obtain a product that has characteristics similar to an industrial Portland clinker?"

The quenched clinker, according to the protocol described in a previous section, was preliminary studied by reflected light microscopy. In order to determine the proportion of each clinker phase, phases were counted on a network of 841 points. Results shown in Table 8 are obtained by volume and converted into mass content by using the density of each phase according to Bye [61].

Reflected Light Microscopy Observations

Clinker nodules prepared with 27.1% SEP and clinker prepared with no substitution of quarried materials were both observed in polished sections. Two micrographs are presented in Figs. 7 and 8, corresponding to the clinker containing SEP sediment and to the clinker produced without sediment, respectively.

As shown on the micrographs, the porosity represents about a third of the total clinker grain volume. This could be explained by the process (granulation before clinkerization). However, observations demonstrate a high proportion of C_3S crystals. Most of them are relatively small (lower than 50 μm). Small alite crystals are known to be more reactive than larger ones [62].

The microscopical phase counting results are presented in Table 8. The calculations are made only on the solid (porosity excluded).

When comparing the results to Pliskin's usual values [60], it can be seen that all the anhydrous phase weight fractions are in the expected ranges. C_3S-to-C_2S ratio is relatively high.

Crystalline phases of the clinker prepared using SEP sediment were also quantified using the Rietveld method. Results are presented in Table 9.

Comparing Tables 8 and 9, it can be observed that alite, belite and tricalcium aluminate contents are similar whatever the quantification technique. The only difference that should be mentioned is the brownmillerite content which is a bit lower when determined by the Rietveld method. With the second method, the crystalline phase composition is in the appropriate range of values according to Pliskin [60], except the alite content which is higher than 70 wt%.

Finally, to assess the combination level of lime with other oxides (mainly silica), free lime is extracted by ethylene–glycol and titrated. Titration shows a mass percentage of 1.18 of free lime, which is a relatively low value. Indeed, referring to [63], Portland cement clinker should contain less than 3 wt% of uncombined calcium oxide. Thus, it can be concluded that a satisfying fraction of the initially incorporated calcium oxide reacted during the clinkerization process. It suggests that the formulation and the lab process were accurate and appropriate—for instance, the raw mix fineness.

As an intermediate conclusion, these preliminary results demonstrate that clinker obtained at the lab scale by substituting 27.1 wt% of the quarried rocks by pre-treated alpine

Table 9 Mineralogical composition of the clinker prepared with SEP sediment by Rietveld method

Clinker phase	C_3S	C_2S	C_3A	C_4AF	Free CaO
Content (wt.%)	71.8	12.0	10.8	5.0	0.4

sediment in the raw mix presents the usual Portland clinker expected characteristics.

Pozzolanic SCM Reuse Option

Materials and Methods

Thermal Activation Process

Clay pozzolanic activation, due to dehydroxylation of clay minerals leading to a collapsed and distorted structure, occurs for temperatures ranging from 550–960 °C depending on the type of clay [64]. Therefore, 10 firing temperatures were tested between 550 and 1000 °C, with a 50 °C step.

Thermal treatment can be divided into three stages. Dried and crushed STA sediment was first heated up to the maximum temperature with a ramp of 5 °C per minute. When the desired temperature was reached, the material was kept for 5 h in the furnace. The crucible was then quenched to room temperature in order to keep the high temperature phases and their structures.

Calcined Products Characterizations

The powders produced by calcination intending to develop a reactivity towards $Ca(OH)_2$ were characterized with the same protocols as the pre-treated sediments. Physical parameters were analysed (PSD, BET SSA, Blaine fineness and pycnometer density) and diffraction patterns were obtained according to the same process. The only difference that should be noticed is the outgassing temperature before BET SSA measurement: it was increased to 200 °C in order to improve the process. Indeed, since the material was previously treated at a temperature higher than 200 °C, there is no alteration risk.

Pozzolanic Activity Assessment

Several protocols for pozzolanic activity assessment could be suggested with direct and indirect methods [65].

In direct methods, the followed parameter is the consumed calcium hydroxide amount due to pozzolanic reaction. It can be done by (i) chemical titration protocols (such as the Frattini test, the Chapelle test and the saturated lime test), (ii) TGA (following the mass loss in lime-pozzolan pastes due to transformation around 550 °C of $Ca(OH)_2$ into CaO) or (iii) XRD (following the intensities and areas of the main peaks corresponding to $Ca(OH)_2$, for instance in lime-pozzolan pastes).

On the other hand, the indirect methods are described as techniques that study another physical parameters that is

assumed to be related to the calcium hydroxide (CH) consumption such as the compressive strength, electrical conductivity and temperature.

In this study, three different methods for the assessment of calcined STA pozzolanic activity were selected:

- One direct method: Frattini test (1), since this titration method is standardized in EN NF 196-5 referring to pozzolanic cements [66];
- Two indirect methodologies: compressive strength tests (2) and semi-adiabatic calorimetry (3).

Each selected protocol is described:

1. Concerning the Frattini test, 20 g of blended cement were prepared mixing 16 g of Ordinary Portland Cement (OPC) and 4 g of calcined sediment (20 wt%). 100 mL of deionized water were added and the samples were stored in sealed plastic containers at 40 °C in order to avoid carbonation reaction. After different curing times (8, 15 and 28 days), the solution was filtrated; free hydroxide and calcium ions concentrations (noted [OH$^-$] and [CaO] in the standard) were immediately determined by colorimetric titration, acid-base titration using 0.1 M HCl and complexation with 0.03 M EDTA, respectively. Concentrations are then plotted in a XY diagram: [CaO] as Y-axis and [OH$^-$] as X-axis.

2. Strength activity index method was used in order to determine the mechanical effect of the calcined sediment additions. Tests were performed on cylindrical cement paste samples (15 mm diameter and 30 mm high) using a 50 kN uniaxial compressive system Instron 5969. Cement pastes were obtained mixing CEM I 52.5 MPa strength class (Portland cement) with 35 wt% of calcined STA at 600 and 900 °C and using a water-to-binder ratio (w/b) equal to 0.5. The SCM content was chosen according to EN NF 197-1 standard [12]: a Portland-composite cement (CEM II) can contain until 35% of SCM. Thus, the chosen replace-

ment ratio meets standard requirements. Moreover, the SCM effect is assumed to be more observable choosing a high substitution ratio of Portland clinker rather than a low one. In order to make a comparative study with other supplementary cementitious materials, strength results with calcined sediments were compared to a calcareous filler (CF) and a silico-aluminous fly ash (FA) using the same replacement ratio (35 wt%). When fly ash is used as clinker replacement in Portland-composite cement, additional hydration products can be expected due to the reaction of FA with the calcium hydroxide dwelling from hydration of OPC [54]. This additional chemical activity has an influence both on mechanical properties [67] and on the heat generated during hydration [68]. Contrary to FA, CF shows only a poor chemical activity. Compared to an OPC hydration, the only complementary reaction that can be noted is the formation carboaluminate hydrates [69]. In contrast to pozzolanic FA addition, the additional strength brought by chemical reaction is relatively poor. The filler effect is mainly physical, with an improvement of particles packing [70]. Thus, calcined STA as SCM is compared to two different poles: FA which is known to be chemically reactive material and CF that has physical properties. Mix proportions are given in Table 10 28 days at 30 °C and >95% relative humidity. A Strength Activity Index (SAI) was calculated according to Eq. 5 as the ratio of the compressive strength of cement paste containing supplementary cementitious material and the compressive strength of a control cement without any addition—Ordinary Portland Cement.

$$SAI = \frac{\sigma_{sample}}{\sigma_{control}} \tag{5}$$

Were σ_{sample} is the compressive strength of the sample containing SCM and $\sigma_{control}$ is the compressive strength of the control sample containing only OPC.

Table 10 Mixture proportions of compressive strength test samples

	w/b (%)	Water (g)	Cement component (g)					
			OPC	PTSTA	600STA	900STA	CF	FA
Control	0.5	225	450					
PTSTA35	0.5	225	292.5	157.5				
600STA35	0.5	225	292.5		157.5			
900STA35	0.5	225	292.5			157.5		
CF35	0.5	225	292.5				157.5	
FA35	0.5	225	292.5					157.5

Symbols for cement components: *OPC* ordinary portland cement, *PTSTA* pre-treated STA, *600STA* STA calcined at 600 °C, *900STA* STA calcined at 900 °C, *CF* calcareous filler, *FA* fly ash

3. Finally, heats of hydration were measured using the semi-adiabatic method (Langavant calorimeter). This technique consists in measuring the cumulative heat generated by cement hydration following the internal cement paste temperature and the room temperature on the same time period. This test was performed during the first 40 h of hydration. Hydration at a given time t, named Q(t) (in Joule per gram of cement) is obtained according to the following Eq. 6:

$$Q(t) = \frac{C_{TOT}}{m_c} \cdot \theta_t + \frac{1}{m_c} \cdot \int_0^t \alpha \cdot \theta_t \cdot dt \qquad (6)$$

Note: In Eq. 6, it is assumed that the generated heat due to cement hydration Q(t) can be divided into 3 parts. One contributes to the temperature increase of the sample, another one to the temperature increase of the calorimeter and the last one is the external heat loss. Thus, C_{TOT} (J/°C) is the total specific heat taking into account the specific heat of the different cement paste compounds and the specific heat of the empty calorimeter, m_c (g) is the cement mass, θ_t (°C) is the temperature difference between the one measured inside the calorimeter and the room temperature, α (J/h/°C) is a coefficient related to the apparatus heat loss. Time t is expressed in hours.

In a blended cement that contains Portland clinker and pozzolan addition, the cumulative released heat can be interpreted as a sum of the heat generated by hydraulic and pozzolanic reactions [71]. Calorimetry test allows a determination of the SCM effect on the cement hydration rate. Similarly to the SAI protocol, sediments calcined at 600 and 900 °C were assessed and compared to the same CF and FA. Calorimetry pastes were prepared using the same OPC replacement ratio i.e. 35% and the same water-to-binder ratio i.e. 0.5.

Results and Discussion

Crystalline Phases and Thermal Treatment

XRD patterns of the crystalline phases according to the calcination temperature are shown in Fig. 9. Pre-treated STA sediment and 3 calcination temperatures (600, 800
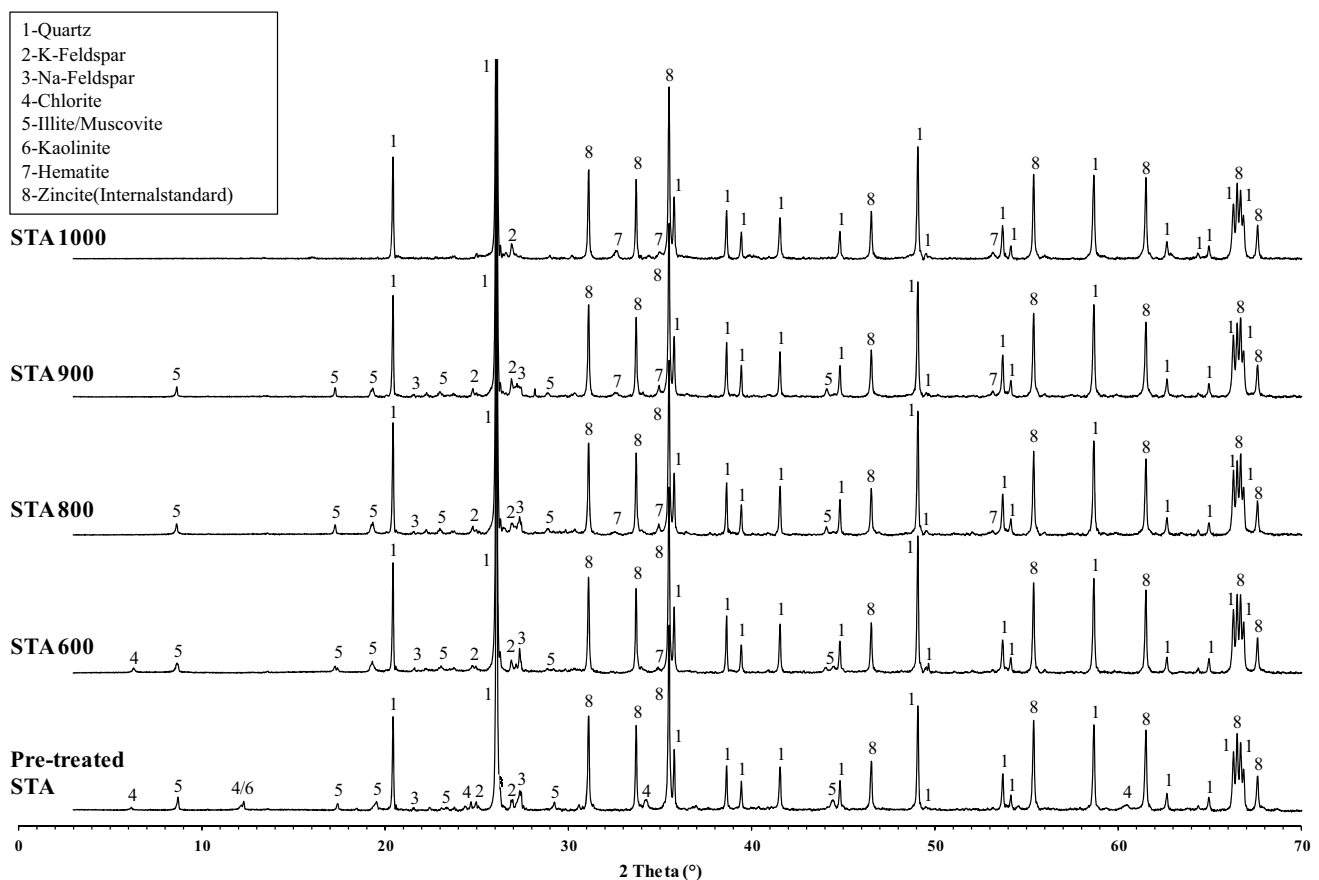

Fig. 9 XRD patterns for 4 different calcination temperatures and comparison to the XRD pattern of the pre-treated sediment

Fig. 10 Summary of the crystalline phase identification at the different calcination temperatures

Temperature (°C)	Mineral phases					
	Quartz	Feldspars	Kaolinite	Chlorite	Illite-Muscovite	Hematite
Pre-treated STA Room temperature						
550°C			✖			
600°C						
650°C				✖		
700°C						
750°C						
800°C						
850°C						(Hematite appears)
900°C						
950°C						
1000°C	↓	↓			✖	↓

✖ : Temperature at which the mineral is no longer identifiable - Extinction

and 950 °C) are given in this diagram. The evolution of the main identified crystalline phases is also presented in Fig. 10 for the ten calcination temperatures.

In Figs. 9 and 10, no change can be seen for quartz. This mineral phases appear relatively stable in the temperature range of 550–1000 °C. Feldspars modifications are observable (position and intensity of peaks). However, feldspars are still present at 1000 °C. The interesting phases to follow are the clay minerals. It is known that heat can dehydroxylate clay phases, resulting in a collapse of the structure. A totally amorphous or partially amorphous material is then obtained. Good pozzolan often presents a high percentage of glass: silica and alumina oxides are available and reactive. They can form binding hydrated phases reacting with calcium hydroxide. It can be observed that kaolinite mineral is dehydroxylated at relatively low temperatures, since the (001) characteristic diffraction peak of kaolinite around 12.3° 2θ has disappeared after calcination at 550 °C. Föld-vari [72] confirmed that the dehydroxylation temperature of kaolinite occurs between 530 and 590 °C. Kaolinite is transformed into amorphous metakaolinite Al_2O_3, $2SiO_2$. According to He et al. [73] this dehydroxylation is directly linked to the pozzolanic activity of the calcined material. Reaction of kaolin calcined at 550 °C is fast and enhanced compared to the raw material. A thermal treatment at higher temperature (up to 800 °C) slightly increases the pozzolanic reactivity. Nevertheless, in the authors' opinion, the gain in reactivity cannot balance the supplementary cost of the heating process. At 950 °C, He et al. observed that there is a loss in reactivity. There is a transition from the amorphous metakaolinite to crystalline mullite. Comparing calcined STA characterization to the literature, it can be confirmed that the kaolinite initially contained in

the dredged material is dehydroxylated under 550 °C, since the (001) peak disappeared after treatment at this calcination temperature. However, no recrystallized phases containing aluminum and silicon oxides can be identified for the highest studied temperatures. Therefore, it can be suggested that the amorphous material formed when structural water of kaolinite is lost, remains in the temperature range of 550–1000 °C.

The second clay mineral that is degraded when the temperature increases is the chlorite phase. At 650 °C, the (001) peak around 7.1° 2θ disappeared, indicating that the chlorite dehydroxylation reaction occurred. Studying calcined waste paper sludge, García et al. [29] also followed the dehydroxylation of the chlorite phase that was mixed with other argillaceous and non-argillaceous minerals. They observed that dehydroxylation of chlorite began at 650 °C and finished at 800 °C. Using DTA analyses, Cook [74] indicated that chlorite was dehydroxylated at 650 °C. To complete this observation, Cook demonstrated that the recrystallization of a pure chlorite clay appeared around 850 °C. Therefore, one can understand that the thermal activation temperature range is quite narrow.

The most thermally stable phyllosilicates contained in pre-treated STA sediment are illite and muscovite. Even if the intensities of the characteristic diffraction peaks diminish when the calcination temperature increases, they are observable until 950 °C. It is necessary to heat the pretreated dredged material to this temperature to fully dehydroxylate illite and muscovite. This high temperature of destruction of the illite crystal lattice is described by several authors. He et al. [75] showed that calcining an illitic clay at 930 °C gave a marked reduction of the XRD peak intensities related to the best pozzolanic activity—assessed

Table 11 Amorphous content of each calcined powder assessed by Rietveld analysis

Temperature (°C)	600	800	900	1000
Amorphous content (wt%)	22.0	21.8	25.5	20.6
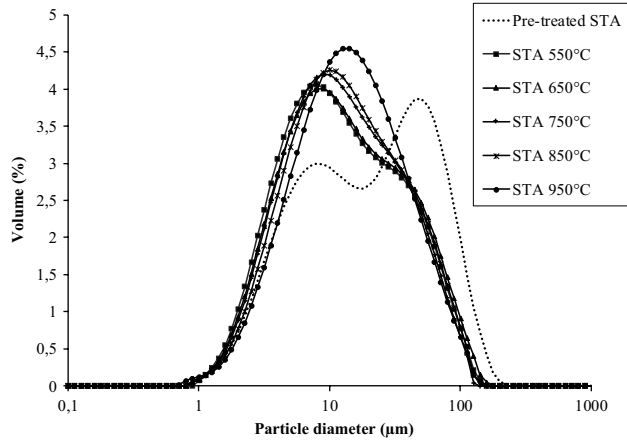
Fig. 11 Particle size distribution of pre-treated and calcined STA

Fig. 12 Density and BET specific surface area according to the calcination temperature of STA sediment

by compressive strength tests on standard mortars. Lemma et al. [69] also worked on calcined illitic clays. They showed by Frattini test that the best pozzolanic activity results are obtained for the highest tested calcination temperature: 950 °C. Again, it corresponds to the most advanced alteration of the illite crystalline structure.

The only mineral recrystallization that could be detected by XRD was hematite. Peaks at 33.3° 2θ, 54.23° 2θ and 35.74° 2θ were barely identifiable at 600 °C. However, their intensity increased with temperature. Identification was more obvious at higher temperatures. Crystallization of hematite after calcination of natural clayey material has already been reported in literature [77, 78].

According to Table 11, Rietveld quantification of the amorphous content demonstrated that it is higher when calcined at 900 °C rather than at the other temperatures. Therefore, this thermal treatment is supposed to lead to a more reactive material.

To summarize these XRD characterizations on samples after treatment at different calcination temperatures, since a mix of clay minerals is initially contained in the pre-treated sediment, it is necessary to consider the activation temperature of all these minerals. A temperature of 900 C appears as an interesting compromise between clay minerals degradation and recrystallization phenomena. Indeed, kaolinite and chlorite degradations are completed and illite intensity is significantly reduced while hematite recrystallization is limited. In accordance with these results, at a temperature of 900 °C, the amorphous content is maximum which is expected when looking for the optimized calcination temperature.

Evolution of the Physical Parameters According to the Calcination Temperature

Four physical characteristics of the calcined powders are described: PSD analyses (given in Fig. 11; Table 12), density, BET specific surface area and Blaine fineness (Fig. 12).

According to the results of Fig. 11 and Table 12, different effects of the thermal treatments on the PSD can be observed:

Table 12 Deciles of the particle size distribution according to the firing temperature

PSD Decile	Pre-treated STA (μm)	STA 550 °C (μm)	STA 650 °C (μm)	STA 750 °C (μm)	STA 850 °C (μm)	STA 950 °C (μm)
d_{10}	4.1	3.5	3.6	3.7	3.9	4.2
d_{50}	21.7	12.2	13.0	12.8	13.6	14.7
d_{90}	83.8	55.2	58.8	52.3	55.4	51.7

i. The pre-treated material shows a bimodal distribution, with a first peak at 5 microns in diameter and a second one, which is higher, at 50 microns. The intensity of this second peak tends to vanish when the powder is heated. It is still observable for firing temperatures of 550 and 650 °C, but can be barely distinguished for calcination temperatures of 750 and 850 °C and is absent for a calcination temperature of 950 °C. For this hottest thermal treatment, the PSD is Gaussian. The observation of a bimodal distribution transformed into a normal distribution after sediment calcination could be explained by the nature of the coarse particles that contribute to the second peak. It is known that STA contains a rather important quantity of organic matter. If the OM fragments are relatively coarse, their oxidation around 300 °C could partly explain the collapse of the second peak

ii. In addition to the change in the shape of the distribution, a second effect of the thermal treatment can be observed. The first mode progressively shifts towards higher diameters when the calcination temperature increases. This effect, combined to the previous one, could be seen as a growth of particles, due to sintering.

In Fig. 12, it can be observed that STA sediment BET SSA evolution presents 3 phases when the temperature increases. First, an increase of BET SSA can be observed when the sediment is calcined at 550 °C compared to the pre-treated sediment. Between 550 and 750 °C, BET SSA remains relatively high, even if a slight decrease is observed from 12.4 m²/g to 10.1 m²/g. Finally, above 750 °C, SSA collapses. At 950 °C, SSA is 2.1 m²/g.

The other followed parameter in Fig. 12, which is the density of the powders, showed an increase by 6% between the pre-treated dredged material and the lowest calcination temperature of 550 °C. It could be linked to the oxidation of organic matter around 300 °C. Indeed, this organic fraction tends to reduce pre-treated sediment density. Since it is degraded before 550 °C, density is relatively higher when the material is calcined. Beyond 550 °C, the density is stable before a thermal treatment at 700 °C. Then, it slightly increases, reaching 2.69 g/cm³ after a thermal treatment at 1000 °C.

To sum up the observations, it can be said that the sintering process begins around 750 °C, leading to particle growth. This phenomenon is associated to a loss in roughness since BET SSA is highly reduced between 750 and 950 °C. This particle growth phenomenon can be correlated to the displacement of the peak in the grain size distribution diagram towards greater values observable in Fig. 11. Considering a Cuban clay, Fernandez-Lopez in 2009 [79] explained the observed BET SSA collapse over 850 °C by

the formation of a liquid phase: particle morphology is modified and new crystalline phases can grow in the porous system. Therefore, a linked explanation to the PSD peak shift could be explained by the newly formed phase—hematite—in addition to the particles agglomeration.

SEM observations on powder mounts were performed in order to determine the effect of temperature on morphology and are presented in Fig. 13. No major evolution in particle size and surface roughness can be detected between the pre-treated material and STA after a thermal treatment at 600 °C. It is in accordance with the BET SSA value which is slightly higher when STA is calcined at 600 °C. However, after a thermal treatment at 900 °C particles present more rounded edges and characteristics of a sintering phenomenon. Surface roughness loss is obvious in accordance with the BET SSA collapse.

As a conclusion on physical characterizations, important changes can be observed in the 550–1000 °C temperature range. These modifications can be related to the mineralogical evolution presented in the previous part, particularly the alteration of clay structures and the formation of crystalline hematite as a new phase due to the thermal treatment above 900 °C. Then, it is necessary to compare previous characterizations on thermal treatment products to pozzolanic activity assessment test, in order to make connections between physical properties and reactivity.

Pozzolanic Activity Assessment

Frattini Test Results

Ca^{2+} and OH^- concentrations of the filtrated solutions from Frattini test are plotted in Fig. 14. On the same diagram, the solubility limit of $Ca(OH)_2$ along with the pozzolanic and non-pozzolanic zones are reported, in accordance with EN NF 196-5 [66].

According to NF EN 196-5 [66], a Portland cement replacement should be considered as a pozzolanic material if the representative dot is located below the $Ca(OH)_2$ solubility curve. It means that the portlandite dwelling from the CEM I hydration is consumed by the Supplementary Cementitious Material (SCM) forming new binding hydrates. Calcium atoms are incorporated into those phases, implying a reduction of calcium ions concentration in the solution in contact with the hardened paste.

Concerning the OPC sample, which should be regarded as the control paste, the evolution is parallel to the solubility curve from 8 to 28 days tending to be more basic with curing time. All the samples prepared with 20 wt% replacement have a lower pH than the control sample.

It can be seen that the pre-treated sediment, even after 28 days of curing, does not demonstrate any pozzolanic
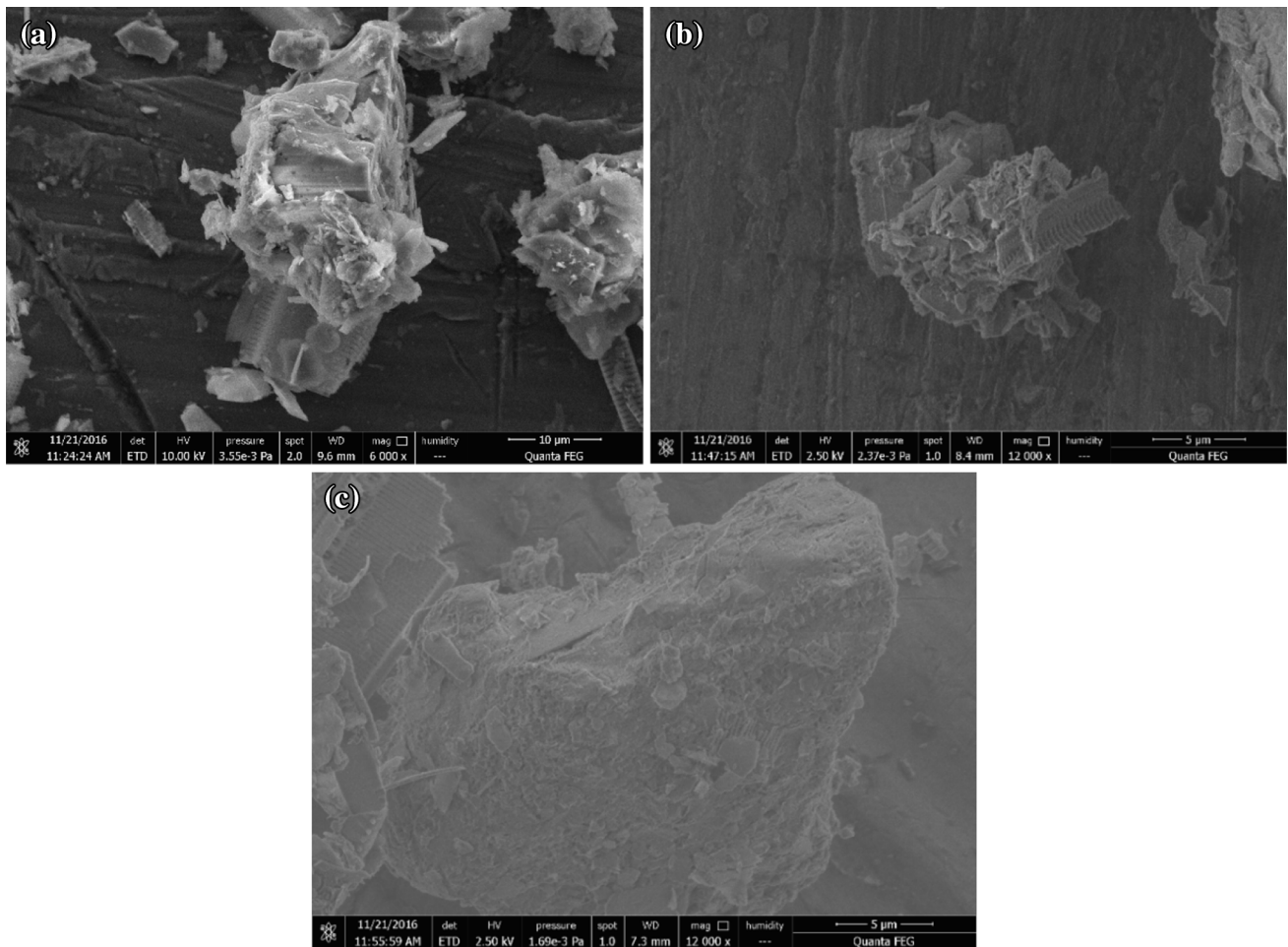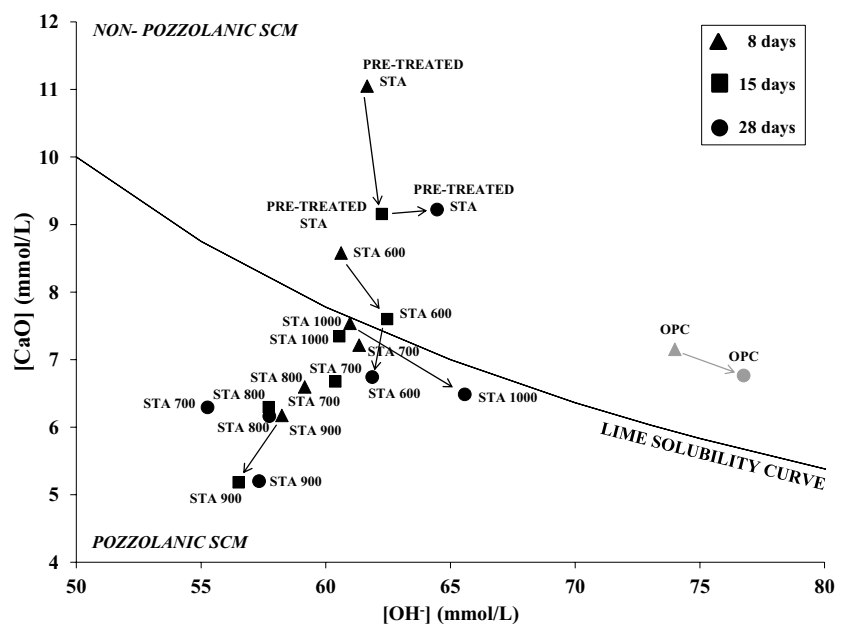
Fig. 13 SEM observations of pre-treated STA **a** and comparison to the calcined materials **b** 600 °C; **c** 900 °C

Fig. 14 Frattini tests results
on pre-treated and thermally
treated STA sediment (*SCM*
supplementary cementitous
material)

effect. However, when the dredged material is thermally treated, all the dots representing the solutions at 28 days are below the saturation curve. Therefore, the Frattini test is positive: adding calcined sediment as a SCM to OPC leads to a removal of calcium ions when the powder is in contact with water. Nevertheless, the extent of calcium removal is quite different according to the firing temperature. Between 600 and 900 °C, the higher the calcination temperature, the greater the calcium removal. Higher than 900 °C, the calcium consumption declines. Dots representing the STA sediment calcined at 1000 °C are close to the solubility curve and the evolution between 8 and 28 days is similar to the control cement paste.

As a conclusion, the Frattini test titration method shows that, contrary to the pre-treated material, all the calcined powders have a pozzolanic reactivity after 28 days of curing. All of them have the property to form hydrated phases consuming the calcium hydroxide released by Portland cement hydration. Therefore, there is a beneficial impact of calcination: the SCM pozzolanic activity is improved.

However, the degree of reaction between lime and SCM varies according to the calcination temperature. The best results are obtained when the material is calcined at 900 °C. As it was mentioned in the mineral characterization, below this temperature, clay minerals are not fully degraded. Above 900 °C, the recrystallization process that occurs, forming hematite, could have a detrimental effect on the reactivity of the material.

Concerning this direct test method, it can be seen that it is a rapid and cost-effective protocol. As it is standardized, it can be considered as reliable and allows a comparison of the studied material to other ones described in scientific papers. This methodology answers the question "does the supplementary cementing material react with calcium hydroxide when water is present?" According to Donatello et al. [80] who confronted different method to

assess the pozzolanic activity of an addition, compressive strength tests results were well correlated to the standard Frattini test. Tironi et al. [81] working on calcined clays, confirmed that there is a good correlation between Frattini test results and Strength Activity Index (SAI) results. However, they also showed that, in some cases, a high chemical consumption of CH by a material in Frattini test is not related to increased mechanical performances.

Hydrates formed by pozzolanic reaction are known to be more variable than hydrates dwelling from Portland cement hydration. Depending on the Al_2O_3/SiO_2 ratio, pozzolanic reaction can lead to various amounts of C–S–H, C–A–S–H and C–A–H phases [61]. For each of them, the formation contributes to lime removal. Thus, it should be checked that lime consumption chemically contributes to strength development.

Considering the consumed $Ca(OH)_2$ using the Frattini test, an optimum calcination temperature can be identified for STA sediment, which is 900 °C. The fixed $Ca(OH)_2$ increases until 900 °C and, at higher temperature, diminishes. Therefore, for semi-adiabatic calorimetry and compressive strength tests only two calcination temperatures are assessed:

- 600 °C that showed a low pozzolanic activity by chemical titration;
- 900 °C which is assumed to be the optimized temperature.

Strength Activity Index

Compressive strengths of cement pastes versus curing time and SAI at 2, 14 and 28 days are presented in Figs. 15 and 16, respectively.

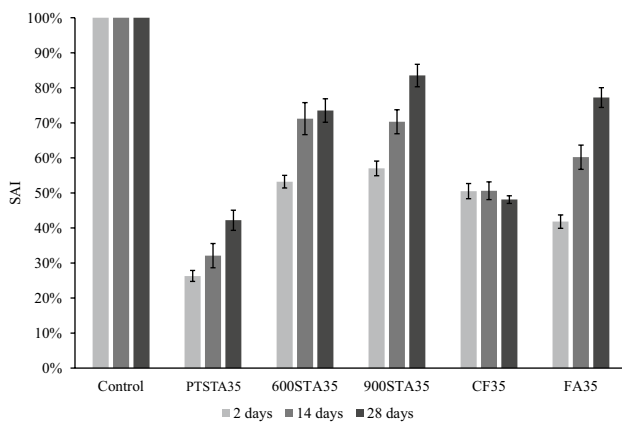Fig. 15 Compressive strengths of cement pastes as a function of time
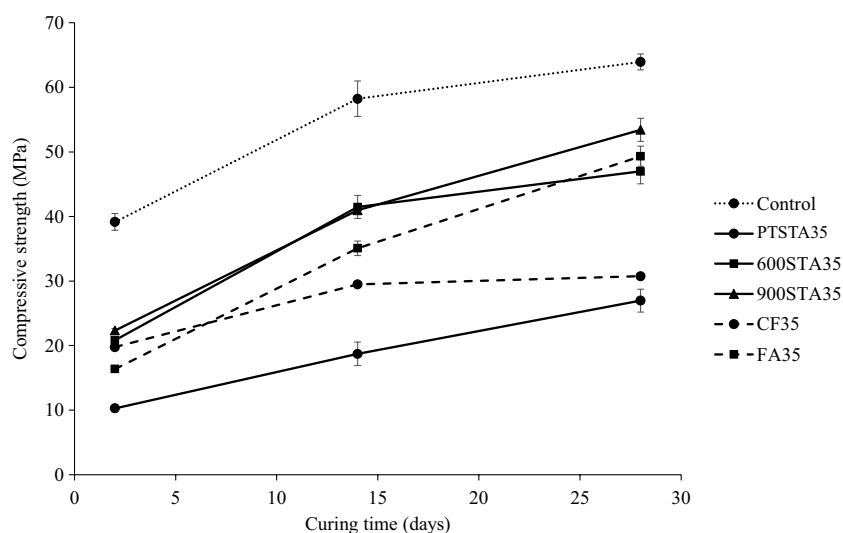
Fig. 16 Strength activity indices of cement pastes after 2, 14 and 28 days of curing

Figure 15 shows that all the cements (with and without mineral additions) show an increase of compressive strength with curing time. This mechanical strength gain is related to the hydration process that occurs during curing time. Hydrates are formed, mainly C–S–H for Portland cement, that lead to hardening and strengthening of the pastes. Whatever the 35 wt% mineral addition, blended cements compressive strengths are lower than the control Portland cement. An explanation for this observation is the dilution effect [82]. As the substitution ratio is high, none of the tested SCM is able to compensate this dilution effect. OPC leads to the formation of hydrated calcium silicates that strengthen the hardened material. Thus, a substitution of this matter by a less active mineral addition in a cement formulation gives lower strength results.

A comparison of compressive strength after 28 days for mixtures PTSTA35, 600STA35 and 900STA35 demonstrates that the best results are obtained for a thermal treatment at 900 °C. Replacing 35 wt% by weight of Portland cement by STA calcined at 900 °C, a cement paste with a SAI equal to 84% is obtained. After a curing period of 28 days, this strength is even higher than the mechanical performances of the blended cement containing FA with the same replacement level. FA material is considered as pozzolanic. Cements incorporating FA usually show slower strength development than OPC [83]. Since dilution effect is partially compensated after 28 days in blended Portland cement containing 900STA with results similar to FA addition with the same replacement level, strength test observations confirmed Frattini test results. The high lime consumption is associated to a strength gain.

28 days strength is diminished by 27% compared to the control sample when the calcination temperature is 300 °C lower. Nevertheless, for 600STA35 mixture, mechanical performances are increased by 74% compared to the uncalcined material. Thus, it can be concluded that

the calcination process is useful. Considering the relatively high organic matter content of the pre-treated STA, an explanation to the poor SAI could be the detrimental impact of OM on both the setting and hardening phenomena [84] combined to the dilution effect. At all curing ages, strength developed by PTSTA35 is lower than the calcareous filler at the same substitution level.

Considering the evolution of the SAI as a function of the curing time in Fig. 16, it can be seen that the highest SAI increases are observed for the most active additions which are FA and 900STA. It is related to the pozzolanic reactivity that is usually slower than the hydraulic one [85].

As a conclusion, strength test results confirm the pozzolanic activity demonstrated by the chemical Frattini test for STA that was calcined at 900 °C. After 28 days, a strength gain can be observed for 900STA compared to the inert filler addition, to STA without thermal treatment, to STA after a calcination at 600 °C and even to the pozzolanic fly ash. As a high replacement ratio was selected in order to accentuate the supplementary cementitious material impact, a dilution effect should be taken into account for each of the substituting materials.

Semi-Adiabatic Calorimetry

Heat of hydration of cement pastes with and without 35 wt% Portland cement replacement by mineral additions are presented in Fig. 17.

At first glance, it clearly appears that the total heat of hydration is diminished when Portland Cement is replaced by 35 wt% of any mineral addition. Quantitatively, after a measuring time of 30 h, the total generated heat is reduced by 27.3% for FA, 31.6% for 900STA, 35.0% for 600STA, 35.5% for PTSTA and 35.7% for CF compared to the control Portland cement paste. Thus, the heat reduction is proportional to the substitution ratio when pre-treated STA, 600STA and calcareous filler are used as supplementary cementitious material. No additional heat is produced by both these additions. Contrary to PTSTA, 600STA and CF additions, FA and 900STA show heat reduction lower than the replacement ratio. Thus, both these supplementary cementitious materials engender heat and should be considered as "active" additions. The diminution of cumulative heat generation during cement hydration when OPC is replaced by FA was also reported by Frías et al. [86]. Same observation can be made for OPC replacement by calcined STA sediment.

Moreover, other interesting results are the curve shapes and the time at which the maximum heat of hydration is reached. Blended cement calorimetry curves are shifted towards greater hydration times compared to the control Portland cement, except for the calcareous filler. This trend

Fig. 17 Heat of hydration of cement pastes
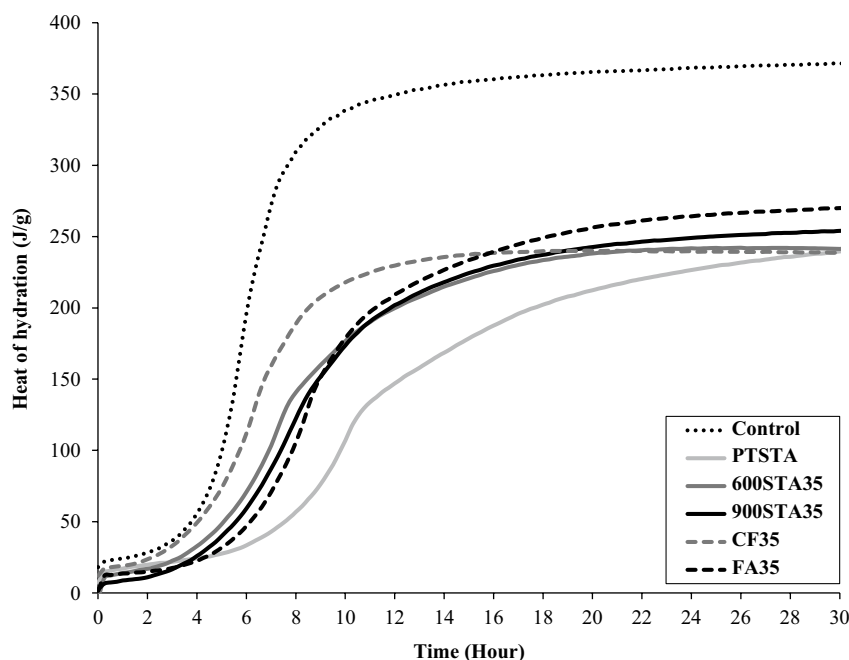
is clearly visible for FA and calcined STA. However, concerning the calcareous filler, the maximum heat of hydration is reached earlier (around 14 h). This hydration acceleration using filler has been reported in literature [87]. This accelerated hydration is explained by the nucleation sites provided by filler addition for C-S-H growth [58, 88]. Concerning 900STA and FA, the additional heat due to pozzolanic reaction is only observed after 16–18 h after the beginning of the experiment. Pre-treated STA significantly modifies hydration reactions. The total heat of hydration reaches its maximum value after 29 h only. Pre-treated STA did not undergo any thermal treatment. Therefore, organic matter remains intact with a known delaying effect on set [89, 90].

To summarize the semi-adiabatic calorimetry results, supplementary heat is generated by 900STA addition when blended with Portland cement (35% by mass replacement) compared to an inert addition. Considering previous results (chemical titration and strength tests), the consumption of portlandite shown by Frattini is correlated to a contribution of 900STA to mechanical strength and to an additional generated heat compared to a chemically inert SCM.

As a conclusion on the beneficial reuse of calcined STA as a supplementary cementitious materials, several correlated results showed that the valorization of this waste is technically feasible. A new cement partially incorporating treated waste instead of manufactured clinker can be formulated. By reducing waste disposal and Portland clinker content in cement, this reuse solution combines two different environmental benefits.

Conclusions

This paper presented a characterization of two dam sediments SEP and STA. The aim of the study was to determine the beneficial reuse potential for each of them in cement industry: SEP as a raw material for clinker production and STA as a pozzolanic addition in blended cements. According to the results, the main conclusions are:

1. STA sediment is a silico-aluminous material, mainly constituted of quartz, K and Na-feldspars and phyllosilicates whereas SEP sediment is more carbonated with a carbonate content around 30%.
2. The pre-treated sediments are fine-grained materials with a d_{50} lower than 63 microns.
3. The total replacement of quarried clay by SEP sediment in clinker raw mix has no major deleterious impact on clinker facies and mineralogical composition.
4. Frattini chemical test results show that lime consumption is optimized when the calcination temperature of STA is 900 °C. Lime consumption increases with temperature between 550 and 900 °C and diminishes when the temperature is 1000 °C. This calcination process optimization was related to the physical and mineralogical evolution of the sediment with temperature. Above 950 °C, a particle growth was observed along with a marked reduction of the BET specific surface area. Pozzolanic reactivity of 900STA is confirmed by SAI results and semi-adiabatic calorimetry results.

Comparing (i) the characteristics of the pre-treated dredged materials to materials used by several authors and similar to ours and (ii) comparing the characteristics of thermally treated products to commercial powders, it can be said that the tested sediments are expected to be technically suitable for the suggested applications. Innovative and more sustainable construction materials are proposed since:

- Partial replacement of the quarried geological rocks to produce clinker by dam sediments would save natural resources;
- The sediment thermal activation would require less energy than the clinkerization of a meal. Thus, by a partial substitution of Portland clinker by activated waste materials, CO_2 efficient binders can be suggested;
- At the same time, waste disposal can be reduced thanks to this industrial ecology approach, complying with the European waste management hierarchy as defined in 2008 in the Waste Framework Directive [9];
- Since waste valorization solutions are technically feasible according to the present study, the remaining and not investigated locks are logistic and industrial. Effective industrial ecology systems could be implemented with dam fine-grained sediment beneficial reuse in the cement industry.

References

1. Jansson M.B.: A global survey of sediment yield. Geogr. Ann. A. **70**, (1/2), 81–98 (1988)
2. Vercruysse, K., Grabowski, R.C., Rickson, R.J.: Suspended sediment transport dynamics in rivers: multi-scale drivers of temporal variation. Earth Sci. Rev. (2017)
3. Gay, A., Cerdan, O., Delmas, M., Desmet, M.: Variability of suspended sediment yields within the Loire river basin (France). J. Hydrol. **519**, 1225–1237 (2014)
4. Udden, J.A.: Mechanical composition of clastic sediment. Geol. Soc. Am. Bull. **25**, 655–744 (1914)
5. Wentworth, C.K.: A scale of grade and class terms for clastic sediments. J. Geol. **30**, 377–392 (1922)
6. Schleiss, J.A.: Sedimentation of reservoirs. In: Bobrowsky, P. T. (ed.) Encyclopedia of natural hazards, pp. 901–905. Springer, Dordrecht (2013)
7. Directive 2000/60/EC of the European Parliament and of the Council of 23 October 2000 establishing a framework for Community action in the field of water policy Official J. Eur. Communities L 327, 1–73 (2000)
8. Law 2006–1772 on Water and Aquatic Environments. Official J. of the French Republic: **303**, 125–177 (2006)
9. Directive 2008/98/EC of the European Parliament and of the Council of 19 November 2008 on waste and repealing certain directives Official J. Eur. Communities L 312, 3–30 (2008)
10. Anger, A.: Characterization of fine-grained sediments from hydroelectric dams reservoirs for an orientation towards beneficial reuse solutions. PhD thesis, University of Caen. 316 p. (2014)
11. Taylor, H.F.W: Cement Chemistry. Academic Press, London (1990)
12. AFNOR. NF EN 197-1. Cement Part 1: Composition, specification and conformity criteria for common cements. 38 p. (2012)
13. Schneider M., Romer M., Tschudin M., Bolio H.: Sustainable cement production-present and future. Cem. Concr. Res. **41**, 642–650 (2011)
14. Huntzinger D N., Eatmon T.D.: A life-cyle assessment of Portland cement manufacturing: comparing the traditional process with alternative technologies. J. Clean. Prod. **17**, 668–675 (2009)
15. De Schepper, M., De Buysser, K., Van Driessche, I., De Belie, N.: The regeneration of cement out of Completely Recyclable Concrete: Clinker production evaluation. Constr. Build. Mater. **38**, 1001–1009 (2013)
16. Puertas, F., García-Díaz, I., Barba, A., Gazulla, M.F., Palacios, M., Gómez, M.P., Martínez-Ramírez, S.: Ceramic wastes as alternative raw materials for Portland cement clinker production. Cem. Concr. Comp. **30**, 798–805 (2008)
17. Iacobescu, R.I., Angelopoulos, G.N., Jones, P.T., Blanpain, B., Pontikes, Y.: Ladle metallurgy stainless steel slag as a raw material in Ordinary Portland Cement production: a possibility of industrial symbiosis. J. Clean. Prod. **112**, 872–881 (2016)
18. Tsakiridis, P.E., Oustadakis, P., Agatzini-Leonardou, S.: Black dross leached residue: An alternative raw material for Portland cement clinker. Waste Biomass Valor. **5**, 973–983 (2014)
19. Buruberri, L.H., Seabra, M.P., Labrincha, J.A.: Preparation of clinker from paper industry wastes. J. Hazard. Mater. **286**, 252–260 (2015)
20. Yen, C.L., Tseng, D.H., Lin, T.T.: Characterization of eco-cement paste produced from waste sludges. Chemosphere. **84**, 220–226 (2011)
21. Xie, Z., Xi, Y.: Use of recycled glass as a raw material in the manufacture of Portland cement. Mater. Struct. **35**, 510–515 (2002)
22. Lin, Y., Zhou, S., Li, F., Yixiao, L.: Utilization of municipal sewage sludge as additives for the production of eco-cement. J. Hazard. Mater. **213–214**, 457–465 (2012)
23. Xu, W., Xu J., Liu J., Li H., Cao B., Huang X., Li G.: The utilization of lime-dried sludge as resource for producing cement. J. Clean. Prod. **83**, 286–293 (2014)
24. Saikia, N., Kato, S., Kojima, T.: Production of cement clinkers from municipal solid waste incineration (MSWI) fly ash. Waste Manage. **27**, 1178–1189 (2007)
25. Lam C.H.K., Barford J.P., McKay G.: Utilization of municipal solid waste incineration ash in Portland cement clinker. Clean Technol. Environ. **13**, 607–615 (2011)
26. Sánchez de Rojas, M.I., Marín, F., Riviera, J., Frías, M.: Morphology and properties in blended cements with ceramic wastes

as a pozzolanic material. J. Am. Ceram. Soc. **89**, 3701–3705 (2006)

27. Medina, C., Sáez del Bosque, I.F., Asensio, E., Frías, M., Sánchez de Rojas, M.I.: Mineralogy and microstructure of hydrated phases during the pozzolanic reaction in the sanitary ware waste/Ca(OH)₂ system. J. Am. Ceram. Soc. **99**, 340–348 (2016)

28. Fernández R., Nebreda B., Vigil de la Villa R., García R., Frías M.: Mineralogical and chemical evolution of hydrated phases in the pozzolanic reaction of calcined paper sludge. Cem. Concr. Comp. **32**, 775–782 (2010)

29. García, R., Vigil de la Villa, R., Vegas, I., Frías, M., Sánchez de Rojas, M.I.: The pozzolanic properties of paper sludge waste. Constr. Build. Mater. **22**, 1484–1490 (2008)

30. Frías M., Villar E., Savastano H.: Brazilian sugar cane bagasse ashes from the cogeneration industry as active pozzolan for cement. Cem. Concr. Comp. **33**, 490–496 (2011)

31. Habeeb G.A., Mahmud H.B.: Study on properties of rice husk ash and its use as cement replacement material. Mater. Res. **13**, 185–190 (2010)

32. Khalil, N.M., Hassan, E.M., Shakdofa M.M.E., Farahat, M.: Beneficiation of the huge waste quantities of barley and rice husks as well as coal fly ashes as additives for Portland cement. J. Ind. Eng. Chem. **20**, 2998–3008 (2014)

33. Frías, M., Vigil de la Villa, R., García, R., Sánchez de Rojas, M.I., Valdés, A.J.: The influence of slate waste activation conditions on mineralogical changes and pozzolanic behavior. J. Am. Ceram. Soc. **96**, 2276–2282 (2013)

34. Zhang, T., Zengzeng, Z.: Optimal use of MSWI bottom ash in concrete. Int. J. Conc. Struc. Mater. **8**, 173–182 (2014)

35. Valenti, G., Bernardo, G., Marroccoli, M., Molino, B.: Beneficial reuse of reservoir sediment in the cement industry. In: Pellei, M., Porta, A.. (eds.) Remediation of contaminated sediments Proceedings of the Second International Conference on Remediation of Contaminated Sediments (Venice, Italy: 30 Sept-3 Oct 2003). Battelle Press, Columbus (2003)

36. Dalton J.L., Gardner K.H., Seager T.P., Weimer M.L., Spear J.C.M., Magee B.J.: Properties of Portland cement made from contaminated sediments. Resour. Conserv. Recycl. **41**, 227–247 (2004)

37. ASTM Standard C150. Standard Specification for Portland Cement. 10 p. (2016)

38. Aouad G., Laboudigue A., Gineys N., Abriak N.E.: Dredged sediments used as novel supply of raw material to produce Portland cement clinker. Cem. Concr. Comp. **32**, 788–793 (2012)

39. Semcha A.: Valorisation des sédiments de dragage - Applications dans le BTP, cas du barrage de Fergoug. PhD Thesis, University of Reims Champagne-Ardenne. 167 p. (2006)

40. Dang, T.A., Kamali-Bernard, S., Prince, W.A.: Design of new blended cement based on marine dredged sediment. Constr. Build. Mater. **41**, 602–611 (2013)

41. Rabehi, B., Ghernouti, Y., Driss, M.: Potential use of calcined silt of dam as a pozzolan in blended Portland cement. Int. J. Concr. Struct. Mater. **8**, 259–268 (2014)

42. Snellings, R., Cizer Ö., Horckmans, L., Durdziński, P.T., Dierckx, P., Nielsen, P., Van Balen, K., Vanderwalle, L.: Properties and pozzolanic reactivity of flash calcined dredging sediments. Appl. Clay Sci. (2016)

43. Brunauer, S., Emmett, P.H., Teller, E.: Adsorption of gases in multimolecular layers. J. Am. Chem. Soc. **60**, 309–319 (1938)

44. Blaine R.L.: A Simplified Air Permeability Fineness Apparatus. Bull. Am. Soc. Test. Mater. **123**, 51–55 (1943)

45. AFNOR NF EN 196-6. Methods of testing cement Part 6: Determination of fineness. 22 p. (2013)

46. Lawrence, C. D.: The Constitution and Specification of Portland Cements. In: Hewlett, P.C. (ed.) Lea's chemistry of cement and concrete 4th Edition, pp. 131–193. Elsevier Science and Technology Books, Oxford (2002)

47. Gualtieri, A.F., Guagliardi, A., Iseppi, A.: The quantitative determination of the crystalline and amorphous content by the Rietveld Method: Application to glass ceramics with different adsorption coefficient. In: Mittemeijer, E.J., Scardi, P.. (eds.) Diffraction Analysis of the Microstructure of Materials, pp. 147–166. Springer, Berlin (2004)

48. AFNOR NF P94-048. Sols: Reconnaissance et essais - Détermination de la teneur en carbonate - Méthode du calcimètre. 11 p. (1996)

49. AFNOR NF EN 12880. Characterization of sludges - Determination of dry residue and water content. 14 p. (2000)

50. Michel F., Courard L.: Particle Size Distribution of Limestone Fillers: Granulometry and Specific Surface Area Investigations. Part. Sci. Technol. **32**, 334–340 (2014)

51. Arvaniti, E.C., Juenger M.C.G., Bernal, S. A., Duchesne, J., Courard, L., Leroy, S., Provis, J.L., Klemm, A., De Belie, N.: Determination of particle size, surface area, and shape of supplementary cementitious materials by different techniques. Mater. Struct. **48**, 3687–3701 (2014)

52. Rankin, G.A., Wright, F.E.: The ternary system lime-alumina-silica. Am. J. Sci. **39**, 1–79 (1915)

53. Aïtcin, P.-C.: Supplementary cementitious materials and blended cements. In: Aïtcin, P.-C., Flatt, R.J.. (eds.) Science and Technology of Concrete Admixtures, pp. 53–73. Woodhead Publishing, Cambridge (2016)

54. Siddique, R., Khan, M.I.: Supplementary cementing materials. Springer, Berlin (2011)

55. Locher, F.W.: Cement: Principles of production and uses. Verlag Bau, Düsseldorf (2006)

56. Kurdowski, W.: Cement manufacture. In: Bensted, J., Barnes, P. (eds.) Structure and performance of cement 2nd Edition, pp. 1–24. Spon Press, London (2002)

57. Campbell D. H.: Microscopical examination and interpretation of Portland cement and clinker Second Edition. Portland Cement Association, Skokie (1999)

58. Neville A.M.: Properties of concrete 5th Edition. Pearson Education Limited, Harlow (2011)

59. Javellana M.P., Jawed I.: Extraction of free lime in portland cement and clinker by ethylene glycol. Cem. Concr. Res. 12, 399–403 (1982)

60. Schläpfer, P., Bukowski, R.: Eidgenössische Materialprüfungsanstalt an der E.T.H. Zürich. Report No. 63. Zurich (1933)

61. Bye, G.C.: Portland Cement Second edition: Composition, Production and Properties. Thomas Telford Publishing, London (1999)

62. Long, G.R.: Clinker Quality Characterization by Reflected Light Techniques. In: Proceedings of the Fourth International Conference on Cement Microscopy, pp. 92–109. Las Vegas (1982)

63. Pliskin, L.: La fabrication du ciment. Eyrolles, Paris (1993)

64. He C., Osbæck B., Makovicky E.: Pozzolanic reactions of six principal clay minerals: activation, reactivity assessments and technological effects. Cem. Concr. Res. **25**, 1691–1792 (1995)

65. Parashar, A., Krishnan, S., Bishnoi, S.: Testing of suitability of supplementary materials mixed in ternary cements. In: Scrivener, K., Favier, A.. (eds.) Calcined Clays for Sustainable Concrete, pp. 419–426. Springer, Dordrecht (2015)

66. AFNOR NF EN 196-5. Methods of testing cement Part 5: Pozzolanicity test for pozzolanic cement. 16 p. (2013)

67. Kocak Y., Nas S.: The effect of using fly ash on the strength and hydration characteristics of blended cements. Constr. Build. Mater **73**, 25–32 (2014)

68. Klemczak, B., Batog, M.: Heat of hydration of low-clinker cements. Part I. Semi-adiabatic and isothermal tests at different temperature. J. Therm. Anal. Calorim. **123**, 1351–1360 (2016)

69. Bonavetti V.L., Rahhal V.F., Irassar E.F.: Studies on the carboaluminate formation in limestone filler-blended cements. Cem. Concr. Res. **31**, 853–859 (2001)

70. Ramezanianpour, A.A.: Cement replacement Materials: properties, durability, sustainability. Springer, Heidelberg (2014)

71. Frías Rojas, M., Sánchez de Rojas Gómez, M.I.: Natural pozzolans in eco-efficient concrete. In: Pacheco-Torgal, F., Jalali, S., Labrincha, J., John, V.M.. (eds.) Eco-efficient concrete, pp. 83–104. Woodhead Publishing Limited, Cambridge (2013)

72. Földvari, M.: Handbook of thermogravimetric system of minerals and its use in geological practice. Hungarian Academy of Sciences, Budapest (2011)

73. He, C., Makovicky, E., Osbæck, B.: Thermal stability and pozzolanic activity of calcined kaolin. Appl. Clay Sci. **9**, 165–187 (1994)

74. Cook, D.J.: Calcined clay, shale and other soils. In: Swamy, R.N. (ed.) Cement replacement materials, pp. 40–72. Surrey University Press, London (1986)

75. He, C., Makovicky, E., Osbæck, B.: Thermal stability and pozzolanic activity of calcined illite. Appl. Clay Sci. **9**, 337–354 (1995)

76. Lemma, R., Irassar, E.F., Rahhal, V.: Calcined illitic clays as Portland cement replacements. In: Scrivener, K., Favier, A.. (eds.) Calcined Clays for Sustainable Concrete, pp. 269–276. Springer, Dordrecht (2015)

77. Alujas, A., Fernández, R., Quintana, R., Scrivener, K.L., Martirena, F.: Pozzolanic reactivity of low grade kaolinitic clays: Influence of calcination temperature and impact of calcination products on OPC hydration. Appl. Clay Sci. **108**, 94–101 (2015)

78. Escalera, E., Tegman, R., Antti, M.-L., Oldén, M.: High temperature phase evolution of Bolivian kaolinitic-illitic clays heated to 1250 °C. Appl. Clay Sci. **101**, 100–105 (2014)

79. Fernandez-Lopez, R.: Calcined clayey soils as a potential replacement for cement in developing countries. PhD thesis, Swiss Federal Institute of Technology Lausanne. 178 p. (2009)

80. Donatello S., Tyrer M., Cheeseman C.R.: Comparison of test methods to assess pozzolanic activity. Cem. Concr. Comp. 32, 121–127 (2010)

81. Tironi A., Trezza M.A., Scian A.N., Irassar E.F.: Assessment of pozzolanic activity of different calcined clays. Cem. Concr. Comp. **37**, 319–327 (2013)

82. Dinakar, P., Sahoo, P. K., Sriram, G.: Effect of metakaolin content on the properties of high strength concrete. Int. J. Concr. Struct. Mater. **7**, 215–223 (2013)

83. Kurdowski, W.: Cement and Concrete Chemistry. Springer, Dordrecht (2014)

84. Eglinton, M.S.: Concrete and its chemical behaviour. Thomas Telford, London (1987)

85. Moir, G.: Cements. In: Newman, J., Choo, B.S. (eds.) Advanced Concrete Technologies, pp. 1/1–1/45. Butterworth-Heinemann, Oxford (2003)

86. Frías, M., Sánchez de Rojas, M.I., Cabrera, J.: The effect that the pozzolanic reaction of metakaolin has on the heat evolution in metakaolin-cement mortars. Cem. Concr. Res. **30**, 209–216 (2000)

87. Soroka I., Stern N.: Calcareous fillers and the compressive strength of Portland cement. Cem. Concr. Res. **6**, 367–376 (1976)

88. Bentz, D.P., Ferraris, C.F., Jones, S.Z., Lootens, D., Zunino, F.: Limestone and silica powder replacements for cement: Early-age performance. Cem. Concr. Comp. (2017)

89. Poole, A., Sims, I.: Geology, aggregates and classification. In: Newman, J., Choo, B.S.. (eds.) Advanced Concrete Technologies, pp. 1/1–1/45. Butterworth-Heinemann, Oxford (2003)

90. Akroyd T.N.W: Concrete: Properties and Manufacture. Pergamon Press Limited, Oxford (1962)